
Graph Neural Networks for Binary Programming

Moshe Eliasof¹ Eldad Haber²

Abstract

This paper investigates a link between Graph Neural Networks (GNNs) and Binary Programming (BP) problems, laying the groundwork for GNNs to approximate solutions for these computationally challenging problems. By analyzing the sensitivity of BP problems, we are able to frame the solution of BP problems as a heterophilic node classification task. We then propose Binary-Programming GNN (BPGNN), an architecture that integrates graph representation learning techniques with BP-aware features to approximate BP solutions efficiently. Additionally, we introduce a self-supervised data generation mechanism, to enable efficient and tractable training data acquisition even for large-scale BP problems. Experimental evaluations of BPGNN across diverse BP problem sizes showcase its superior performance compared to exhaustive search and heuristic approaches. Finally, we discuss open challenges in the under-explored field of BP problems with GNNs.

1. Introduction

Solving *Binary Programming* (BP) Problems is of paramount importance in optimization and decision-making. These problems, characterized by binary decision variables, arise in numerous real-world scenarios, such as portfolio optimization (Black & Litterman, 1992), manufacturing and supply chain optimization (Geunes & Pardalos, 2005), telecommunications network optimization (Resende & Pardalos, 2008), resource allocation (Brown, 1984) and more. As the name suggests, Binary Programming (BP) is a type of mathematical problem where decision variables are restricted to take binary values (0 or 1). The discrete nature of BP makes these problems computationally challenging. Specifically, BP problems are known to be NP-complete (Karp, 2010). However, the solution of

BP problems is crucial for optimizing the allocation of resources and improving operational efficiency. Contemporary solutions involve a range of optimization techniques, ranging from relaxation techniques and linear programming solvers (Nowak, 2005) to heuristic algorithms and heuristic-based approaches (Merz & Freisleben, 2002). Emerging technologies, such as quantum computing, show promise in addressing BP problems more efficiently (Glover et al., 2018), offering novel avenues for optimization in the future. However, they are not readily available yet, and their current setups are limited to solving problems with a small number of decision variables.

Concurrently, in recent years, Graph Neural Networks (GNNs) have emerged as powerful machine learning models, and have been applied to various domains and applications, from social network analysis (Kipf & Welling, 2016; Defferrard et al., 2016; Veličković et al., 2018), bioinformatics (Jumper et al., 2021), to computer vision and graphics (Monti et al., 2017; Hanocka et al., 2019), and more.

In this paper, we show that it is possible to model Binary Programming problems as a graph learning problem, namely node classification. Our findings lay the ground for leveraging the power of Graph Neural Networks in approximating the solutions of BP problems. Importantly, by characterizing the solution landscape of BP problems, we show that their solutions can be interpreted as *heterophilic* node classification. Therefore, we propose *BPGNN*, a Binary-Programming GNN, that builds on recent advances in heterophilic node classification with BP-aware features as part of its architecture. Another important aspect when using GNNs (or other data-driven techniques) to solve BP problems, is the scarcity of labeled data. While it is possible to use exhaustive search models to generate solutions of problems with a low number of decision variables, generating data for more than a dozen of decision variables becomes computationally intractable. We therefore propose a data generation procedure that stems from our theoretical analysis of the behavior of the solution landscape of BP problems. Our novel approach not only seeks to bridge the gap between traditional BP and cutting-edge neural graph representation learning techniques, but also holds the potential to offer more efficient and effective methodologies for addressing a wide range of computationally demanding optimization problems in diverse applications.

*Equal contribution ¹University of Cambridge ²University of British Columbia. Correspondence to: Moshe Eliasof <me532@cam.ac.uk>.

Contributions: This paper makes several contributions on multiple fronts. (i) It establishes a novel connection that links between Graph Neural Networks and Binary Programming problems. This key observation serves as the foundation for exploring the utilization of GNNs in addressing and approximating solutions to computationally hard problems. (ii) We conduct a sensitivity analysis of the Binary Programming problems with respect to the input variables. This analysis sheds light on patterns and behavior of the solutions of BP learning problems, providing an understanding on how to address these problems using GNNs, by treating the solution of BP learning problems as heterophilic node classification. (iii) We propose an efficient self-supervised mechanism for generating training data, to address the NP-complete problem of generating data using exhaustive search otherwise. Finally, (iv) we evaluate BPGNN on varying sizes of BP problems and compare its performance with exhaustive search, heuristic, and other GNN approaches. Collectively, these contributions advance the understanding and utilization of GNNs in the realm of Binary Programming, paving the way for novel and efficient approaches to address this problem.

2. Problem Formulation

In this work, we consider BP problems and focus on the solution of the family of Quadratic Unconstrained Binary Optimization (*QUBO*) problems:

$$\mathbf{x}_o = \arg \min_{\mathbf{x} \in \{0,1\}^k} f(\mathbf{x}; \mathbf{b}, \mathbf{A}) = \mathbf{x}^\top \mathbf{A} \mathbf{x} + \mathbf{x}^\top \mathbf{b}, \quad (1)$$

where $\mathbf{x} \in \mathbb{B}^k$ is a binary decision variables vector, $\mathbf{A} \in \mathbb{R}^{k \times k}$ is a real-valued matrix and $\mathbf{b} \in \mathbb{R}^k$ is a given real-valued vector, also sometimes called the observed vector. The QUBO problem was thoroughly studied in the literature, and we refer to (Beasley, 1998; Kochenberger et al., 2014; Glover et al., 2018) and reference within for theoretical as well as practical algorithms for its solution.

Obtaining exact solutions for QUBO problems is computationally challenging and limited, due to their discrete nature. As we discuss in Section 3, many heuristic-based methods have been proposed to solve this problem. However, despite such heuristics, it is still evident that in many cases, it is difficult to obtain a reasonable solution in polynomial time (Kochenberger et al., 2014), especially in high dimensions. In this work we focus on approximating the QUBO solution in a polynomial time for a subset of QUBO problems, assuming that the matrix \mathbf{A} is sparse and fixed, but the observed vector \mathbf{b} can vary. Such problems arise in virtually any field where QUBO problems are utilized (Black & Litterman, 1992; Geunes & Pardalos, 2005; Resende & Pardalos, 2008; Brown, 1984). For these problems, the matrix \mathbf{A} represents the interaction between the variables, and the vector \mathbf{b} is data that varies.

An important observation that we make is that QUBO can be interpreted as a graph problem. Let us consider a graph $G = (V, E)$ with a set of k nodes, V , and a set of m edges, E . The matrix $\mathbf{A} \in \mathbb{R}^{k \times k}$ from Equation (1) can be interpreted as the adjacency matrix of a graph G . The connectivity of G is therefore represented by the sparsity pattern of \mathbf{A} , and the edge weights are represented by the matrix values. In the context of graphs and GNNs, we can treat \mathbf{b} from Equation (1) as the input node features.

With this observation, we are motivated to explore the utilization of Graph Neural Networks (GNNs) to approximate the solution of QUBO problems. We show that through this approach, it is possible to efficiently obtain approximations to the solutions of the QUBO problem.

3. Related Work

We now shortly review related work within both QUBO solvers and GNN architectures.

3.1. Popular Binary Programming Solution Techniques

Solving QUBO problems has a wide and rich algorithmic treatment that ranges from exhaustive search methods, relaxation methods, differential equations based approaches, and grid search methods. We refer the reader to (Beasley, 1998) and more recently to (Goto et al., 2019) for a review of the algorithms. We now provide an overview of existing methods, focusing on representative methods that approximate a solution to the QUBO problem in Equation (1). We chose these techniques because they are publicly available and commonly used in literature Oshiyama & Ohzeki (2022).

Exhaustive Search. Overall, the QUBO problem has 2^k plausible solutions. While not always practical, the simplest approach is to use an exhaustive search. That is, test each of the possible solutions and choose the one that achieves the minimal value of Equation (1). This approach is viable when k is small, but it becomes restrictive as k grows. For instance, a problem of size $k = 1024$ has 2^{1024} plausible solutions, making exhaustive search impractical.

Tabu Search (TS). Is a family of iterative algorithms that start from some initial guess \mathbf{x}_0 , and defines a list, \mathcal{T} of maximum length ℓ , dubbed the Tabu list, that is initialized as with \mathbf{x}_0 . The algorithm then defines a list of neighbors, \mathcal{N} of \mathbf{x}_0 as perturbations in various policies (Beasley, 1998; Glover & Laguna, 1998; Glover et al., 2018). The simplest perturbation policy is defined as a vector $\tilde{\mathbf{x}}_{(i)}$ whose entries are identical to \mathbf{x}_0 , with the exception of the i -th index. The neighbors list is then compared to the Tabu list and repeated entries are excluded from the neighbors list. That is, at iteration $t + 1$ we can write, $\mathcal{N}_{t+1} = \mathcal{N}_t \setminus \mathcal{T}_t$. The objective function is then evaluated on all the neighbors and

the solution is updated according to

$$\tilde{\mathbf{x}}_{t+1} = \arg \min_{\tilde{\mathbf{x}} \in \mathcal{N}_t} \tilde{\mathbf{x}}^\top \mathbf{A} \tilde{\mathbf{x}} + \tilde{\mathbf{x}}^\top \mathbf{b}. \quad (2)$$

The Tabu list is then updated, adding \mathbf{x}_{t+1} to it and, possibly omitting the $\mathbf{x}_{t-\ell}$ term from it. The Tabu algorithm performs the described procedure for T steps and returns the approximation vector with the lowest value obtained in the search. Note that each step in TS requires $\mathcal{O}(k)$ function evaluations. Although such an approach does not guarantee a global solution, it tends to yield low approximation error.

Simulating Adiabatic Bifurcations (SAB). A different approach that has been developed recently based on differential equations and molecular dynamics is SAB (Goto et al., 2019). In this approach, the decision variables in \mathbf{x} are relaxed to be continuous, and a Hamiltonian function that has binary stationary points is minimized by simulating the dynamics to a steady state. This process is also known as annealing. In this approach, the cost of each step is a single matrix-vector product. However, as is typical with annealing methods, many steps are needed to reach convergence.

As the problem size, k , grows, it becomes difficult to obtain the exact solution with either TS or SAB (Oshiyama & Ohzeki, 2022). Furthermore, as we show in our experiments in Section 7, their computation time is high, making predictions in real time impractical using these approaches.

3.2. Graph Neural Networks

Graph Neural Networks (GNNs) were introduced in Scarselli et al. (2008) and became popular in recent years after advances in Defferrard et al. (2016); Kipf & Welling (2016). GNNs were shown to be effective in various applications and fields. A non-exhaustive list includes computer vision (Monti et al., 2017; Hanocka et al., 2019; Wang et al., 2018), social network analysis in semi-supervised settings (Kipf & Welling, 2016; Veličković et al., 2018), bioinformatics (Jumper et al., 2021; Corso et al., 2023). Essentially, GNNs allow the processing and learning from unstructured data described by graphs, to solve tasks such as node classification and graph classification, among other tasks. We refer the interested reader to Wu et al. (2020); Waikhom & Patgiri (2023) for a comprehensive review.

In this paper, we propose to use GNNs as a computational model to accelerate the solution approximation of BP problems, by viewing the problem as a heterophilic node classification task. We elaborate on this perspective in Section 4. Node classification problems are now a common application of GNNs (Kipf & Welling, 2016; Veličković et al., 2018; Pei et al., 2020; Chen et al., 2020; Chamberlain et al., 2021). It is common to categorize node classification problems into *homophilic* and *heterophilic*, or non-homophilic types. To define homophily and heterophily, we follow the definition

in Pei et al. (2020), which measures the ground-truth label similarity of neighboring nodes. As shown in Gasteiger et al. (2019); Chamberlain et al. (2021), diffusion-based GNNs are useful for homophilic graphs, where neighboring nodes have similar labels. However, heterophilic node classification is deemed as a more challenging problem, and has been extensively studied in recent years. For example, some methods propose to learn both low and high pass filters (Chien et al., 2021; Luan et al., 2022; Eliasof et al., 2023b), while other methods focus on taking inspiration from neural ordinary differential equations (Haber et al., 2017; Chen et al., 2018) to incorporate operators that allow to model heterophilic behavior. Some recent examples are ACMP (Wang et al., 2022) and GREAD (Choi et al., 2023) that use reaction and diffusion terms to generate non-smooth patterns, as well as methods like CDE (Zhao et al., 2023) that utilize convection-diffusion dynamics, and ADR-GNN that uses advection-diffusion-reaction terms (Eliasof et al., 2023a). Other approaches include graph rewiring (Li et al., 2023), as well as learning directional message passing neural networks in Dir-GNN (Rossi et al., 2023). In the next section, we describe how a QUBO problem is transformed into a heterophilic node classification problem, and how to leverage the power of GNNs to solve such problems.

On another note, a recent line of works under the theme of Neural Algorithmic Reasoning (Veličković & Blundell, 2021; Ibarz et al., 2022; Bevilacqua et al., 2023) suggests to train a neural network to replicate the exact behavior of polynomial complexity algorithms. In this work, however, we seek to accelerate the computation of approximated solutions to the NP-complete QUBO problem.

4. From Combinatorial Optimization to Graph Learning Problems

In this section, we lay the foundation and assumptions of the proposed approach in this paper that shows how a difficult optimization problem can be approximated by learning to solve a node classification problem. We then analyze the characteristics of the node classification problem to be solved, showing its connection with heterophilic graphs.

4.1. Assumptions

Let \mathbf{x}_o be the solution of the optimization problem in Equation (1). Given \mathbf{b} , computing the exact solution requires solving an NP-complete optimization problem (Karp, 2010). Thus, it is common to compromise on an approximation solution, that can be obtained by classical solvers as described in Section 3. Still, those solvers require significant computational time and resources. We will now show that we are able to approximate the solutions using a neural approach, harnessing the power of GNNs.

Proposition 4.1. *Given the observed vector $\mathbf{b} \in \mathbb{R}^k$, there is a piece-wise differentiable function $q : \mathbb{R}^k \rightarrow \mathbb{B}^k$ that maps the vector \mathbf{b} to a binary solution vector $\mathbf{x}_o \in \mathbb{B}^k$.*

Let us assume that we have n solved problems, for different observation vectors. Thus, we have observation-solution pairs $\{\mathbf{b}^{(j)}, \mathbf{x}_o^{(j)}\}$, $j = 0, \dots, n-1$. Then, following Proposition 4.1, we suggest that we can approximate the function $q : \mathbb{R}^k \rightarrow \mathbb{B}^k$ via a neural network. Specifically, in the context of GNNs, the observed vector \mathbf{b} and the solution \mathbf{x}_o can be thought of as node features and labels, respectively. The graph connectivity, i.e., adjacency matrix, is defined by the sparsity of the matrix \mathbf{A} . Because our goal is to map every node to a binary value (0 or 1), the problem of learning the map q can be formulated as a node classification problem, a common application of GNNs (Kipf & Welling, 2016).

4.2. Properties of the BP Problem

As stated in Proposition 4.1, we seek to utilize a node classification GNN to approximate BP solutions. Therefore, and in light of our discussion about homophilic and heterophilic datasets in Section 3.2, it is important to understand the properties of the solutions that we wish to approximate. We now analyze the sensitivity of the solution \mathbf{x}_o with respect to the observed vector \mathbf{b} .

The Landscape of the Map $q(\cdot)$. To justify the ability to learn a map, $q : \mathbb{R}^k \rightarrow \mathbb{B}^k$, from the observed vector \mathbf{b} to the BP solution, \mathbf{x}_o , we need to understand the behavior of the function $q(\mathbf{b})$, and its sensitivity to changes in \mathbf{b} . While such analysis is not known to us for the general case, there are specific problems with physical interpretation that are thoroughly studied, as discussed in Example 1.

Example 1 (The Ising model solution sensitivity is piece-wise constant). *Consider the Ising model with constant coefficients (Dziarmaga, 2005; Duminil-Copin & Tassion, 2016), that reads:*

$$I(\mathbf{x}, \mathbf{A}, \mathbf{b}) = \mathbf{x}^\top \mathbf{A} \mathbf{x} - b \mathbf{x}^\top \mathbf{e}, \quad (3)$$

where \mathbf{e} is a vector of ones, the matrix \mathbf{A} is binary and b is a scalar. The solution, \mathbf{x}_o , remains fixed for a continuous range of b , and it changes rapidly at some b_c that is called the critical value. That is, in this case of the Ising model, we have that $d\mathbf{x}_o/db$ is a piece-wise constant function.

To further analyze the solution of the problem in a more general manner, we start by proving the following theorem:

Theorem 4.2. *The BP problem in Equation (1), at its optimum, i.e., $f(\mathbf{x}_o)$, is piece-wise differentiable with respect to changes of the observed vector \mathbf{b} .*

Proof. Let us define the function

$$f(\mathbf{x}, \epsilon) = \mathbf{b}^\top \mathbf{x} + \mathbf{x}^\top \mathbf{A} \mathbf{x} + \epsilon \boldsymbol{\delta}^\top \mathbf{x}. \quad (4)$$

where $\|\boldsymbol{\delta}\| = 1$ is a direction vector. Let \mathbf{x}_ϵ be the minimizer of Section 4.2 and let $f_\epsilon = f(\mathbf{x}_\epsilon, \epsilon)$. Then, by the definition of the minimizer, we have that for any ϵ

$$f_0 + \epsilon \boldsymbol{\delta}^\top \mathbf{x}_\epsilon \leq f(\mathbf{x}_\epsilon, 0) + \epsilon \boldsymbol{\delta}^\top \mathbf{x}_\epsilon = f(\mathbf{x}_\epsilon, \epsilon) = f_\epsilon \quad (5)$$

Similarly, we have that:

$$\begin{aligned} f_\epsilon &= f(\mathbf{x}_\epsilon, \epsilon) \\ &\leq f(\mathbf{x}_0, \epsilon) = f(\mathbf{x}_0, 0) + \epsilon \boldsymbol{\delta}^\top \mathbf{x}_0 = f_0 + \epsilon \boldsymbol{\delta}^\top \mathbf{x}_0. \end{aligned} \quad (6)$$

This means that we can bound f_ϵ as follows:

$$f_0 + \epsilon \boldsymbol{\delta}^\top \mathbf{x}_\epsilon \leq f_\epsilon \leq f_0 + \epsilon \boldsymbol{\delta}^\top \mathbf{x}_0. \quad (7)$$

Subtracting f_0 from both sides and dividing by ϵ and assuming $0 < \epsilon$ we obtain that

$$\boldsymbol{\delta}^\top \mathbf{x}_\epsilon \leq \frac{f_\epsilon - f_0}{\epsilon} \leq \boldsymbol{\delta}^\top \mathbf{x}_0. \quad (8)$$

Because the norms of \mathbf{x}_0 and \mathbf{x}_ϵ are bounded (as they are binary) we obtain upper and lower bounds for the change in the optimal solution in the direction $\boldsymbol{\delta}$. This is the definition of Clarke derivative (Michel & Penot, 1992), which extends the definition of the derivative beyond a point to an interval. The function $f(\mathbf{b})$ is therefore piece-wise linear. \square

Theorem 4.2 shows that the BP problem in Equation (1) is piece-wise differentiable with respect to \mathbf{b} , a property that we now utilize in order to characterize the BP solution behavior with respect changes in the observed vector \mathbf{b} .

Observation 4.3. The BP solution is piece-wise constant with respect to changes in \mathbf{b} .

Proof. To study the effect of a change in \mathbf{b} on the solution \mathbf{x}_ϵ we now choose $\boldsymbol{\delta} = \mathbf{e}_j$, that is, the unit vector in direction j . This simplifies Equation Section 4.2 to

$$\epsilon \mathbf{x}_{\epsilon_j} \leq \epsilon \mathbf{x}_{0_j}, \quad (9)$$

where the j stands for the j -th entry in the vector. Recall that \mathbf{x} gets only binary values. If, $\epsilon > 0$, $\mathbf{x}_{0_j} = 0$ and $\mathbf{x}_{0_j} \neq \mathbf{x}_{\epsilon_j}$ then we must have that $\mathbf{x}_{\epsilon_j} = 1$, which yields a contradiction. This implies that $\mathbf{x}_{0_j} = \mathbf{x}_{\epsilon_j}$, $\forall \epsilon > 0$.

Furthermore, in this case $f_0 = f_\epsilon$ which implies that $\mathbf{x}_0 = \mathbf{x}_\epsilon$ is a solution of the perturb problem. Thus we obtain that

$$\frac{\delta \mathbf{x}_{0_j}}{\epsilon^+} = 0 \quad \text{if } \mathbf{x}_{0_j} = 0. \quad (10)$$

Similarly, if $\mathbf{x}_{0_j} = 1$ and $\epsilon < 0$ and $\mathbf{x}_{\epsilon_j} \neq \mathbf{x}_{\epsilon_j}$, then $\mathbf{x}_{\epsilon_j} = 0$. But this again yields a contradiction which means

$$\frac{\delta \mathbf{x}_{0_j}}{\epsilon^-} = 0 \quad \text{if } \mathbf{x}_{0_j} = 1. \quad (11)$$

This implies that the function $q(\cdot)$ is piece-wise constant with respect to changes in \mathbf{b} . \square

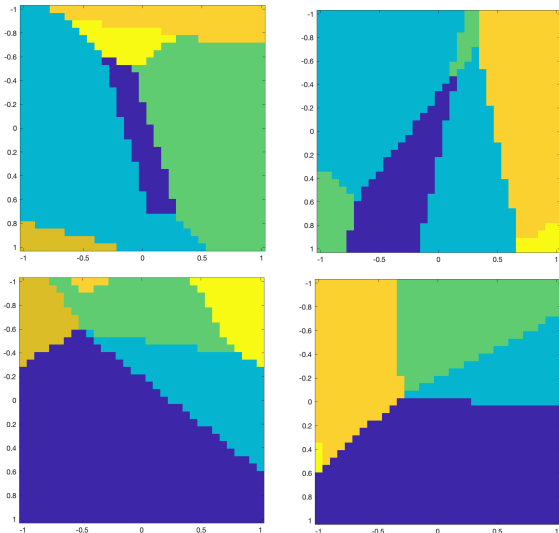


Figure 1. The function $\phi(s, t)$ in Example 2 for four different random realizations of \mathbf{A} , \mathbf{b} , \mathbf{b}_1 and \mathbf{b}_2 . $\phi(s, t)$ is piece-wise constant, favored by neural networks.

Below, in Example 2, we provide a concrete example of this property, and showcase its piece-wise constant landscape behavior with respect to the vector \mathbf{b} .

Example 2. Let us randomly choose $\mathbf{A} \in \mathbb{R}^{20 \times 20}$ and $\mathbf{b} \in \mathbb{R}^{20}$. We compute the exact solution \mathbf{x}_0 using exhaustive search. We then choose two random orthogonal directions \mathbf{b}_1 and \mathbf{b}_2 . Using these fixed vectors we find the solution

$$\mathbf{x}(s, t) = \operatorname{argmin}_{\mathbf{x}} (\mathbf{b} + t\mathbf{b}_1 + s\mathbf{b}_2)^\top \mathbf{x} + \mathbf{x}^\top \mathbf{A} \mathbf{x}. \quad (12)$$

For each $\mathbf{x}(s, t)$ we compute the distance

$$\phi(s, t) = \|\mathbf{x}(s, t) - \mathbf{x}(0, 0)\|^2. \quad (13)$$

In Figure 1 we plot ϕ as a function of s and t for four different experiments where the matrix, \mathbf{A} , the vector, \mathbf{b} and the perturbations \mathbf{b}_1 and \mathbf{b}_2 are randomly chosen. In all cases, we see that the solution is constant over a range of values and then sharply changes. Such surfaces are good candidates for deep network approximation.

5. Approximating BP Solutions with GNNs

Section 4 discusses the ability to learn the map $\mathbf{x}_0 = q(\mathbf{b})$, as well as the characteristics of this map. In this section, we explore the behavior of the solution vector \mathbf{x} , which hints about the needed type of map. We then propose an appropriate architecture to approximate the map.

5.1. The Heterophilic Behavior of BP Solutions

While it is difficult to predict the exact distribution of the solution \mathbf{x} , a few simple cases have been studied in the context

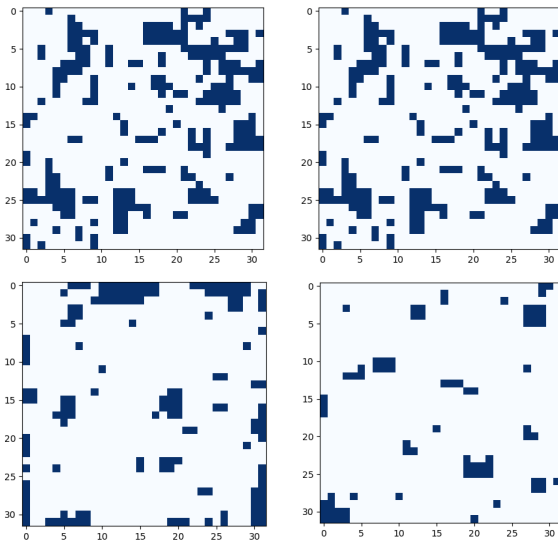


Figure 2. The solution \mathbf{x}_0 for different random values of the vector \mathbf{b} . The graph in this example is a regular lattice where each node (pixel) i, j is connected to its 4 neighbors.

of the Ising model (Dziarmaga, 2005). For this model, it is known that when the solution resides on a regular lattice, it can exhibit high-frequency patterns. In graphs and GNNs, such solutions are commonly affiliated with heterophily (Pei et al., 2020; Choi et al., 2023). To demonstrate that, we solve four different problems on a lattice of size 32×32 using the SAB algorithm (Goto et al., 2019) and plot the solutions in Figure 2. It is observed that the obtained solutions are highly irregular and contain small connected components of uniform values. This implies that typical graph diffusion, or smoothing-based GNNs may face difficulties in expressing such non-smooth patterns. Therefore, as we show in Section 5.2, we leverage the power of heterophily-designated GNNs, combined with a specialized BP-aware component.

5.2. Binary Programming Graph Neural Network

In Section 5.1 and Figure 2 we established that the spatial behavior of the solution of the BP problem, \mathbf{x}_0 , is heterophilic. In this section, we design a GNN that is capable of generating spatially non-smooth patterns while being aware of its application – predicting approximations of BP solutions.

GNN Backbone. In recent years, many heterophily-designated GNN architectures have been proposed. A non-exhaustive list includes (Zhu et al., 2020; Luan et al., 2022; Rusch et al., 2022; Eliasof et al., 2023b; Wang et al., 2022; Choi et al., 2023; Zhao et al., 2023; Rossi et al., 2023). In this paper, we chose to use a reaction-diffusion based network, which is similar to ACMP (Wang et al., 2022) and GREAD (Choi et al., 2023). Our motivation for following this approach is that it is inspired by Turing patterns (Turing,

1952), which are complex and have relation to the Ising model (Merle et al., 2019), which is an instance of a BP problem, as discussed in Example 1. We note that while other heterophilic designated architectures can be used, this is not the focus of our work. Rather, our contribution is drawing the link between GNNs, node classification, and the solution of Binary Programming problems.

QUBO Objective Awareness. While the chosen reaction-diffusion GNN is powerful (also as shown in our experiment in Section 7.2), we argue that it is important also to allow the network to be aware of the objective we seek to minimize, that is, the QUBO function, as shown in Equation (1). To this end, note that the QUBO objective can be written as the sum of the nodal residual of the vector $\mathbf{r} = \mathbf{x} \odot (\mathbf{A}\mathbf{x} + \mathbf{b})$, where \odot is the Hadamard product. Thus, we add the following term to the node features at each layer:

$$\mathbf{r}^{(\ell)}(\mathbf{h}^{(\ell)}, \mathbf{A}, \mathbf{b}) = \mathbf{h}^{(\ell)} \odot (\mathbf{A}\mathbf{h}^{(\ell)} + \mathbf{b}), \quad (14)$$

This modification allows the network to implicitly track the nodal QUBO loss, allowing the network to be aware of the optimization problem at hand. As we show in Section 7.2, this addition improves the solution approximation and training convergence, as we show in our experiments.

BPGNN. Given input features \mathbf{b} , we first embed them to obtain the initial features using a Multilayer Perceptron (MLP) encoder denoted by enc , as follows:

$$\mathbf{h}^{(0)} = \text{enc}(\mathbf{b}) \in \mathbb{R}^{k \times d}. \quad (15)$$

We denote a GNN backbone layer by $\text{GNN}^{(\ell)}$, which takes as input the node features at the ℓ -th layer, $\mathbf{h}^{(\ell)}$, and outputs updated node features $\mathbf{h}^{(\ell+1)}$, i.e.,:

$$\mathbf{h}^{(\ell+1)} = \text{GNN}^{(\ell)}(\mathbf{h}^{(\ell)}). \quad (16)$$

As described in Equation (14), we also include QUBO objective awareness. Thus, a BPGNN layer reads:

$$\mathbf{h}^{(\ell+1)} = \text{GNN}^{(\ell)}(\mathbf{h}^{(\ell)} + g^{(\ell)}(\mathbf{r}^{(\ell)})), \quad (17)$$

where g is an MLP. As discussed earlier, for our GNN implementation we use a reaction-diffusion GNN, discussed in Appendix A. Since we consider a binary problem, after L layers, we use a decoder (classifier) denoted dec , implemented by a linear layer to obtain the predicted solution:

$$\mathbf{x}_p = \text{dec}(\mathbf{h}^{(L)}) \in \mathbb{R}^{k \times 1}. \quad (18)$$

6. Generating Training Data

In order to train the network, given a matrix \mathbf{A} , we require to have observation-solution pairs $\{\mathbf{b}^{(j)}, \mathbf{x}_o^{(j)}\}$, $j = 0, \dots, n-1$. Given these pairs, we use the binary cross-entropy loss

function between $\mathbf{x}_p^{(j)}$, the predicted solution obtained from BPGNN, and the ground-truth solution $\mathbf{x}_o^{(j)}$.

Data Acquisition is Computationally Expensive. An important aspect is how data pairs observation-solution pairs $\{\mathbf{b}^{(j)}, \mathbf{x}_o^{(j)}\}$ can be obtained. Because, as discussed throughout the paper, given an observation vector $\mathbf{b}^{(j)}$, finding the optimal solution $\mathbf{x}_o^{(j)}$ is an NP-complete problem. For small problems (e.g., $k \leq 20$) one can use exhaustive search techniques. This approach requires solving the optimization problem in order to obtain a training set. Clearly, such an approach cannot be used for large-scale problems. For example, if $k = 1024$, one has to check 2^{1024} possible solutions.

Practical Data Pairs Generation. In light of the computational challenge described above, we derive a novel data generation technique. Specifically, instead of choosing the observed vector $\mathbf{b}^{(j)}$ and then solving an NP-complete problem to find $\mathbf{x}_o^{(j)}$, we choose first $\mathbf{x}_o^{(j)}$, and only then find a corresponding $\mathbf{b}^{(j)}$. This procedure allows to create data pairs while avoiding the solution of an NP-complete problem. Specifically, we consider a relaxed optimization problem, where \mathbf{x} is *continuous* in the interval $[0, 1]$:

$$\min_{\mathbf{x} \in [0,1]} \mathbf{x}^\top \mathbf{A}\mathbf{x} + \mathbf{x}^\top \mathbf{b}. \quad (19)$$

One popular way to solve this minimization problem is by the *log barrier* approach (Nocedal & Wright, 1999), which is obtained by adding the logarithmic terms as follows:

$$\min \mathbf{x}^\top \mathbf{A}\mathbf{x} + \mathbf{x}^\top \mathbf{b} - \mu \sum (\log \mathbf{x} + \log(1 - \mathbf{x})). \quad (20)$$

As shown in Nocedal & Wright (1999), the conditions for a minimum are:

$$(\mathbf{A} + \mathbf{A}^\top)\mathbf{x} + \mathbf{b} - \frac{\mu}{\mathbf{x}} + \frac{\mu}{1 - \mathbf{x}} = 0. \quad (21)$$

Now, suppose that we pick \mathbf{x}_o randomly to be $\{\epsilon, 1 - \epsilon\}^k$, where ϵ is small and define \mathbf{b} as follows:

$$\mathbf{b}_o = -(\mathbf{A} + \mathbf{A}^\top)\mathbf{x}_o + \frac{\mu}{\mathbf{x}_o} - \frac{\mu}{1 - \mathbf{x}_o}, \quad (22)$$

$$\mathbf{b} = \mathbf{b}_o + \sigma^2 \mathbf{z}, \quad (23)$$

where $\mathbf{z} \sim N(0, \mathbf{I})$ is a random vector. The vector \mathbf{b}_o corresponds to an approximate solution to the optimization problem in Section 6, which is also the solution of the binary problem in Equation (1). By adding a noise term $\sigma^2 \mathbf{z}$ to the observed vector in Section 6, the solution of the continuous optimization problem is now different from the solution of the discrete binary problem. Nonetheless, as explored in the previous section, the solution of the discrete problem varies little when σ is not large. We therefore use a small number of Tabu search steps, starting from \mathbf{x}_o to modify the solution

Algorithm 1 Practical Data Generation

Input: Problem size k , Variance σ , Matrix \mathbf{A} , parameter $\mu = 10^{-3}$.

Output: Data pair (\mathbf{b}, \mathbf{x}) .

- 1: Randomly choose $\mathbf{x}_o \in \{\epsilon, 1 - \epsilon\}^k$.
- 2: Set $\mathbf{b}_o = -(\mathbf{A} + \mathbf{A}^\top)\mathbf{x}_o + \frac{\mu}{\mathbf{x}_o} - \frac{\mu}{1 - \mathbf{x}_o}$.
- 3: Perturb $\mathbf{b} \leftarrow \mathbf{b}_o + \sigma^2 \mathbf{z}$, where $\mathbf{z} \sim N(0, \mathbf{I})$.
- 4: Use up to ten Tabu search iterations to solve Equation (1) starting from \mathbf{x}_o to obtain improved an solution \mathbf{x} .
- 5: Return (\mathbf{b}, \mathbf{x}) .

if needed. While there is no guarantee that the solution is minimal, we have verified by comparison with exhaustive search solutions on small-scale problems that indeed we obtain the global minima every time. This approach, of choosing \mathbf{x}_o rather than \mathbf{b} allows us to quickly generate large amounts of data even for large-scale problems (with hundreds or thousands of decision variables), where finding the exact solution is computationally intractable. Our procedure for data generation is summarized in Algorithm 1.

7. Numerical Experiments

In this section, we evaluate the performance of BPGNN and other baselines to understand whether our theoretical observations regarding the behavior of the BP, characterized in Section 4.2 and Section 5.1, hold in practice.

Baselines. We consider several baselines in our experiments: (i) naive methods, i.e., exhaustive search, (ii) classical solvers such as TS (Glover & Laguna, 1998) and SAB (Goto et al., 2019), and (iii) GNN baselines, namely GCN (Kipf & Welling, 2016), GAT (Veličković et al., 2018), GCNII (Chen et al., 2020), and Dir-GNN (Rossi et al., 2023). We chose to compare our method with those baselines as they are popular and represent methods from recent years in the context of GNNs. Also, Dir-GNN is heterophily designated, thus suitable to be tested with the heterophilic behavior of BP solutions, as discussed in Section 5.1.

Metrics. In our experiments, we consider three important metrics: (i) the solution accuracy (higher is better), (ii) the *relative* QUBO objective value (lower is better), and (iii) the computation time required to achieve the approximated solution. We elaborate on the metrics in Appendix B.

Datasets. Our experiments include three datasets generated by our procedure described in Section 6, in varying sizes - small ($k = 10$), medium ($k = 256$) and large ($k = 1024$). Note that the settings of $k = \{256, 1024\}$ are considered highly challenging, as there are $2^{\{256, 1024\}}$ possible solutions to the binary programming problem. We provide further details on the datasets in Appendix C.

Implementation. Our code is implemented in Pytorch

(Paszke et al., 2019) and Pytorch-Geometric (Fey & Lenssen, 2019).

Inference. We consider two main inference modes to obtain an approximation of the solutions of BP problems.

- **Neural.** As standard in neural networks, we employ BPGNN to approximate the QUBO solution.
- **Hybrid.** We obtain a solution approximation using BPGNN. This solution is considered an initial point in a classical solver. In our experiments, we used a small *fixed* number (up to 10) iterations of TS (Glover & Laguna, 1998), as discussed in Section 3.1.

7.1. QUBO Solution Approximation

We now compare the obtained solution using the various baselines, as previously discussed. Our results are reported in Table 1. We report results on small, medium, and large datasets. As discussed in 2, here we consider the case where the adjacency matrix \mathbf{A} from Equation (1) is constant, while the observed vector \mathbf{b} is variable. To ensure the statistical significance of our results, for each problem size, we generate 10 instances of the problem matrix \mathbf{A} and report the average and standard deviation metrics in Table 1 and E.1.

Our results indicate that: (i) Naturally, an exhaustive search yields an accurate solution. However, it is not practical for medium or large problems (i.e., as the number of decision variables k , or nodes in the context of GNNs, grows). (ii) Classical solvers achieve impressive accuracy on small problems. However, the accuracy degrades as the problem grows, and the required computational time significantly grows. (iii) GNNs are capable of modeling the considered QUBO problem, effectively learning the discussed map $q(\cdot)$ in Section 4. We also see that in accordance with our understanding regarding the behavior of BP solutions, heterophily designated GNNs such as Dir-GNN and our BPGNN offer higher accuracy and a lower relative QUBO objective compared to other GNNs. (iv) Combining neural approaches, such as our BPGNN, together with classical solvers as TS, offers improved performance, at a fraction of the cost of approximating the problem solution with classical solvers from scratch. Therefore, we deem that our approach can also serve as a strong prior to initializing classical solvers.

7.2. QUBO Aware Features Improve Performance

As presented in Equation (14), our BPGNN includes QUBO-aware node features, which is a novel component of our approach. Therefore, we now examine its impact on the performance. In Table 2, we report the results. It can be seen that including QUBO-aware features adds negligible computation time (less than a millisecond) while improving solution accuracy, on average, by 1.7% and reducing the

Method ↓ / Problem Size →	Small ($k = 10$)			Medium ($k = 256$)			Large ($k = 1024$)		
	Acc(%)	Rel. QUBO Objective	Inference Time (ms)	Acc(%)	Rel. QUBO Objective	Inference Time (ms)	Acc(%)	Rel. QUBO Objective	Inference Time (ms)
NAIVE APPROACH.									
Exhaustive Search	100	0	8	100	0	10^7 days	100	0	10^{302} days
CLASSICAL SOLVERS.									
TS	98.2 ± 0.1	$5.90 \cdot 10^{-3}$	439	96.4 ± 0.3	$4.72 \cdot 10^{-3}$	2197	93.9 ± 0.2	$4.58 \cdot 10^{-3}$	4409
SAB	100	0	298	91.4 ± 0.2	$5.38 \cdot 10^{-2}$	5340	89.2 ± 0.4	$7.96 \cdot 10^{-2}$	40007
GNN BASELINES.									
GCN	70.7 ± 2.4	$7.12 \cdot 10^{-1}$	2.8	69.4 ± 2.8	$5.03 \cdot 10^{-1}$	2.9	62.7 ± 2.8	$8.76 \cdot 10^{-1}$	9.0
GAT	71.3 ± 1.3	$6.98 \cdot 10^{-1}$	3.0	79.7 ± 1.4	$4.38 \cdot 10^{-1}$	3.2	65.5 ± 1.7	$7.23 \cdot 10^{-1}$	12.9
GIN	74.4 ± 2.8	$6.02 \cdot 10^{-1}$	2.8	73.1 ± 1.5	$4.19 \cdot 10^{-1}$	2.9	71.6 ± 1.7	$6.20 \cdot 10^{-1}$	9.2
GCNII	75.1 ± 3.4	$5.67 \cdot 10^{-1}$	2.6	87.1 ± 1.9	$4.13 \cdot 10^{-1}$	2.9	81.6 ± 2.1	$5.08 \cdot 10^{-1}$	9.1
Dir-GNN	89.6 ± 0.6	$3.74 \cdot 10^{-2}$	2.8	90.0 ± 0.7	$1.07 \cdot 10^{-1}$	3.1	89.2 ± 0.4	$9.62 \cdot 10^{-2}$	10.3
OURS.									
BPGNN	98.2 ± 0.5	$2.83 \cdot 10^{-3}$	2.8	97.2 ± 0.4	$5.31 \cdot 10^{-3}$	3.0	93.7 ± 0.5	$1.26 \cdot 10^{-2}$	10.1
BPGNN + TS	98.4 ± 0.3	$1.37 \cdot 10^{-5}$	17	97.4 ± 0.3	$1.21 \cdot 10^{-5}$	194	94.5 ± 0.2	$1.10 \cdot 10^{-4}$	746

Table 1. A quantitative comparison between a naive exhaustive search method, classical methods, GNNs, and our BPGNN.

QUBO Features	Large ($k = 1024$)		
	Acc(%)	Rel QUBO Objective	Inference Time (ms)
✗	91.7 ± 0.8	$6.18 \cdot 10^{-2}$	9.3
✓	93.7 ± 0.5	$1.26 \cdot 10^{-2}$	10.1

Table 2. The impact of adding the QUBO aware features from Equation (14) to the node features.

relative QUBO objective by a factor of almost 2, and improving training convergence, as we show in Appendix E.2.

8. Limitations and Open Challenges

The experiments above demonstrate our ability to train a network to solve the QUBO problem Equation (1) for a **fixed** matrix \mathbf{A} and a variable vector \mathbf{b} . Our theoretical observations and empirical findings pave the way to further research in the connection between solving complex combinatorial problems such as BP problems using GNNs. We now provide several possible significant extensions of our work, both theoretically and in practical applications.

Variable Adjacency Matrix \mathbf{A} . A first open challenge is to extend this work to the case where the matrix \mathbf{A} is also allowed to change, which is an important problem, see for example (Oshiyama & Ohzeki, 2022) for non-neural solutions. This aspect is important because it allows to model different underlying problems and graphs, rather than only a variable observed vector \mathbf{b} .

Constrained Problems. In this paper, we consider QUBO,

which is a subset of unconstrained binary optimization problems. However, many binary problems require considering constraints. Several examples are the knapsack problem (Kellerer et al., 2004), topology optimization (Sivapuram & Picelli, 2018), and protein design (Strokach et al., 2020).

Nonquadratic Problems. In this paper, we study the approximation of QUBO problems using GNNs, but future research can also consider nonquadratic problems, for example, (Murray & Ng, 2010) used in applications such as protein design (Allouche et al., 2014) and telecommunication network optimization (Resende & Pardalos, 2008).

9. Summary

This paper introduces a novel approach, merging graph learning and optimization problem-solving, with an innovative perspective on approximating combinatorial problems solutions by using GNNs. We analyze the input-output relationship of QUBO problems and show that their sensitivity is piecewise constant, and their solutions are heterophilic. These insights guide the design of BPGNN, a GNN architecture to approximate input-solution mappings.

To efficiently generate input-solution data pairs, we propose a novel and scalable mechanism that enables data generation while avoiding the solution of the NP-complete QUBO problem from scratch. Our Numerical results affirm the superiority of BPGNN in accuracy for fixed graph problems, outperforming other GNN solutions while improving computational efficiency compared to classical solvers.

Furthermore, this work not only establishes and evaluates the link between GNNs and BP problems, but also outlines promising future research directions in this emerging

research area.

Impact Statement

This paper presents work whose goal is to advance the field of Machine Learning. We believe it draws an important link between the approximation of the solution of NP-complete problems and neural networks, specifically by utilizing Graph Neural Networks. This work is a first step in this direction and we discuss important future directions. The success and growth of this research front can positively impact various fields, from bioinformatics, to finance, logistics, and more. We are not aware of negative societal consequences of our work.

References

- Allouche, D., André, I., Barbe, S., Davies, J., de Givry, S., Katsirelos, G., O’Sullivan, B., Prestwich, S., Schiex, T., and Traoré, S. Computational protein design as an optimization problem. *Artificial Intelligence*, 212:59–79, 2014.
- Beasley, J. E. Heuristic algorithms for the unconstrained binary quadratic programming problem. Technical report, Working Paper, The Management School, Imperial College, London, England, 1998.
- Bevilacqua, B., Nikiforou, K., Ibarz, B., Bica, I., Paganini, M., Blundell, C., Mitrovic, J., and Veličković, P. Neural algorithmic reasoning with causal regularisation. *arXiv preprint arXiv:2302.10258*, 2023.
- Black, F. and Litterman, R. Global portfolio optimization. *Financial analysts journal*, pp. 28–43, 1992.
- Brown, T. C. The concept of value in resource allocation. *Land economics*, 60(3):231–246, 1984.
- Chamberlain, B. P., Rowbottom, J., Gorinova, M., Webb, S., Rossi, E., and Bronstein, M. M. Grand: Graph neural diffusion. *arXiv preprint arXiv:2106.10934*, 2021.
- Chen, M., Wei, Z., Huang, Z., Ding, B., and Li, Y. Simple and deep graph convolutional networks. In III, H. D. and Singh, A. (eds.), *Proceedings of the 37th International Conference on Machine Learning*, volume 119 of *Proceedings of Machine Learning Research*, pp. 1725–1735. PMLR, 13–18 Jul 2020. URL <http://proceedings.mlr.press/v119/chen20v.html>.
- Chen, T. Q., Rubanova, Y., Bettencourt, J., and Duvenaud, D. K. Neural ordinary differential equations. In *Advances in Neural Information Processing Systems*, pp. 6571–6583, 2018.
- Chien, E., Peng, J., Li, P., and Milenkovic, O. Adaptive universal generalized pagerank graph neural network. In *International Conference on Learning Representations*, 2021. URL <https://openreview.net/forum?id=n6jl7fLxrP>.
- Choi, J., Hong, S., Park, N., and Cho, S.-B. Gread: Graph neural reaction-diffusion networks. In *International Conference on Machine Learning*, pp. 5722–5747. PMLR, 2023.
- Corso, G., Stärk, H., Jing, B., Barzilay, R., and Jaakkola, T. S. Diffdock: Diffusion steps, twists, and turns for molecular docking. In *The Eleventh International Conference on Learning Representations*, 2023. URL https://openreview.net/forum?id=kKF8_K-mBbS.
- Defferrard, M., Bresson, X., and Vandergheynst, P. Convolutional neural networks on graphs with fast localized spectral filtering. In *Advances in neural information processing systems*, pp. 3844–3852, 2016.
- Duminil-Copin, H. and Tassion, V. A new proof of the sharpness of the phase transition for bernoulli percolation and the ising model. *Communications in Mathematical Physics*, 343:725–745, 2016.
- Dziarmaga, J. Dynamics of a quantum phase transition: Exact solution of the quantum ising model. *Physical review letters*, 95(24):245701, 2005.
- Eliasof, M., Haber, E., and Treister, E. PDE-GCN: Novel architectures for graph neural networks motivated by partial differential equations. *Advances in Neural Information Processing Systems*, 34:3836–3849, 2021.
- Eliasof, M., Haber, E., and Treister, E. Adr-gnn: Advection-diffusion-reaction graph neural networks. *arXiv preprint arXiv:2307.16092*, 2023a.
- Eliasof, M., Ruthotto, L., and Treister, E. Improving graph neural networks with learnable propagation operators. In *International Conference on Machine Learning*, pp. 9224–9245. PMLR, 2023b.
- Evans, L. C. *Partial Differential Equations*. American Mathematical Society, San Francisco, 1998.
- Fey, M. and Lenssen, J. E. Fast graph representation learning with PyTorch Geometric. In *ICLR Workshop on Representation Learning on Graphs and Manifolds*, 2019.
- Gasteiger, J., Weißenberger, S., and Günnemann, S. Diffusion improves graph learning. In *Conference on Neural Information Processing Systems (NeurIPS)*, 2019.
- Geunes, J. and Pardalos, P. M. *Supply chain optimization*, volume 98. Springer Science & Business Media, 2005.
- Glover, F. and Laguna, M. *Tabu search*. Springer, 1998.

- Glover, F., Kochenberger, G., and Du, Y. A tutorial on formulating and using qubo models. *arXiv preprint arXiv:1811.11538*, 2018.
- Goto, H., Tatsumura, K., and Dixon, A. R. Combinatorial optimization by simulating adiabatic bifurcations in nonlinear hamiltonian systems. *Science advances*, 5(4): eaav2372, 2019.
- Gravina, A., Bacciu, D., and Gallicchio, C. Anti-symmetric dgn: a stable architecture for deep graph networks. *arXiv preprint arXiv:2210.09789*, 2022.
- Haber, E., Ruthotto, L., Holtham, E., and Jun, S.-H. Learning across scales - A multiscale method for convolution neural networks. abs/1703.02009:1–8, 2017. URL <http://arxiv.org/abs/1703.02009>.
- Hanocka, R., Hertz, A., Fish, N., Giryas, R., Fleishman, S., and Cohen-Or, D. Meshcnn: a network with an edge. *ACM Transactions on Graphics (TOG)*, 38(4):90, 2019.
- Ibarz, B., Kurin, V., Papamakarios, G., Nikiforou, K., Benani, M., Csordás, R., Dudzik, A. J., Bošnjak, M., Vitvitskiy, A., Rubanova, Y., et al. A generalist neural algorithmic learner. In *Learning on Graphs Conference*, pp. 2–1. PMLR, 2022.
- Jumper, J., Evans, R., Pritzel, A., Green, T., Figurnov, M., Ronneberger, O., Tunyasuvunakool, K., Bates, R., Žídek, A., Potapenko, A., et al. Highly accurate protein structure prediction with alphafold. *Nature*, 596(7873):583–589, 2021.
- Karp, R. M. *Reducibility among combinatorial problems*. Springer, 2010.
- Kellerer, H., Pferschy, U., Pisinger, D., Kellerer, H., Pferschy, U., and Pisinger, D. *Multidimensional knapsack problems*. Springer, 2004.
- Kingma, D. P. and Ba, J. Adam: A method for stochastic optimization. *arXiv preprint arXiv:1412.6980*, 2014.
- Kipf, T. N. and Welling, M. Semi-supervised classification with graph convolutional networks. *arXiv preprint arXiv:1609.02907*, 2016.
- Kochenberger, G., Hao, J.-K., Glover, F., Lewis, M., Lü, Z., Wang, H., and Wang, Y. The unconstrained binary quadratic programming problem: a survey. *Journal of combinatorial optimization*, 28:58–81, 2014.
- Li, S., Kim, D., and Wang, Q. Restructuring graph for higher homophily via adaptive spectral clustering. In *Proceedings of the AAAI Conference on Artificial Intelligence*, volume 37, pp. 8622–8630, 2023.
- Luan, S., Hua, C., Lu, Q., Zhu, J., Zhao, M., Zhang, S., Chang, X.-W., and Precup, D. Revisiting heterophily for graph neural networks. *Conference on Neural Information Processing Systems*, 2022.
- Merle, M., Messio, L., and Mozziconacci, J. Turing-like patterns in an asymmetric dynamic ising model. *Phys. Rev. E*, 100:042111, Oct 2019. doi: 10.1103/PhysRevE.100.042111. URL <https://link.aps.org/doi/10.1103/PhysRevE.100.042111>.
- Merz, P. and Freisleben, B. Greedy and local search heuristics for unconstrained binary quadratic programming. *Journal of heuristics*, 8:197–213, 2002.
- Michel, P. and Penot, J.-P. A generalized derivative for calm and stable functions. 1992.
- Monti, F., Boscaini, D., Masci, J., Rodola, E., Svoboda, J., and Bronstein, M. M. Geometric deep learning on graphs and manifolds using mixture model cnns. In *Proceedings of the IEEE Conference on Computer Vision and Pattern Recognition*, pp. 5115–5124, 2017.
- Murray, W. and Ng, K.-M. An algorithm for nonlinear optimization problems with binary variables. *Computational optimization and applications*, 47(2):257–288, 2010.
- Nocedal, J. and Wright, S. *Numerical Optimization*. Springer, New York, 1999.
- Nowak, I. *Relaxation and decomposition methods for mixed integer nonlinear programming*, volume 152. Springer Science & Business Media, 2005.
- Oshiyama, H. and Ohzeki, M. Benchmark of quantum-inspired heuristic solvers for quadratic unconstrained binary optimization. *Scientific reports*, 12(1):2146, 2022.
- Paszke, A., Gross, S., Massa, F., Lerer, A., Bradbury, J., Chanan, G., Killeen, T., Lin, Z., Gimelshein, N., Antiga, L., Desmaison, A., Kopf, A., Yang, E., DeVito, Z., Raison, M., Tejani, A., Chilamkurthy, S., Steiner, B., Fang, L., Bai, J., and Chintala, S. Pytorch: An imperative style, high-performance deep learning library. In Wallach, H., Larochelle, H., Beygelzimer, A., d'Alché-Buc, F., Fox, E., and Garnett, R. (eds.), *Advances in Neural Information Processing Systems 32*, pp. 8024–8035. Curran Associates, Inc., 2019.
- Pei, H., Wei, B., Chang, K. C.-C., Lei, Y., and Yang, B. Geom-gcn: Geometric graph convolutional networks. In *International Conference on Learning Representations*, 2020. URL <https://openreview.net/forum?id=S1e2agrFvS>.
- Resende, M. G. and Pardalos, P. M. *Handbook of optimization in telecommunications*. Springer Science & Business Media, 2008.

- Rossi, E., Charpentier, B., Giovanni, F. D., Frasca, F., Günnemann, S., and Bronstein, M. Edge directionality improves learning on heterophilic graphs, 2023.
- Rusch, T. K., Chamberlain, B. P., Mahoney, M. W., Bronstein, M. M., and Mishra, S. Gradient gating for deep multi-rate learning on graphs. *arXiv preprint arXiv:2210.00513*, 2022.
- Scarselli, F., Gori, M., Tsoi, A. C., Hagenbuchner, M., and Monfardini, G. The graph neural network model. *IEEE transactions on neural networks*, 20(1):61–80, 2008.
- Sivapuram, R. and Picelli, R. Topology optimization of binary structures using integer linear programming. *Finite Elements in Analysis and Design*, 139:49–61, 2018.
- Strokach, A., Becerra, D., Corbi-Verge, C., Perez-Riba, A., and Kim, P. M. Fast and flexible protein design using deep graph neural networks. *Cell Systems*, 11(4):402 – 411.e4, 2020. ISSN 2405-4712. doi: <https://doi.org/10.1016/j.cels.2020.08.016>. URL <http://www.sciencedirect.com/science/article/pii/S2405471220303276>.
- Turing, A. M. The chemical basis of morphogenesis. *Phil. Transact Royal Soc. B*, 37:237–242, 1952.
- Veličković, P. and Blundell, C. Neural algorithmic reasoning. *Patterns*, 2(7), 2021.
- Veličković, P., Cucurull, G., Casanova, A., Romero, A., Liò, P., and Bengio, Y. Graph Attention Networks. *International Conference on Learning Representations*, 2018. URL <https://openreview.net/forum?id=rJXMpikCZ>.
- Waikhom, L. and Patgiri, R. A survey of graph neural networks in various learning paradigms: methods, applications, and challenges. *Artificial Intelligence Review*, 56(7):6295–6364, 2023.
- Wang, Y., Sun, Y., Liu, Z., Sarma, S. E., Bronstein, M. M., and Solomon, J. M. Dynamic graph cnn for learning on point clouds. *arXiv preprint arXiv:1801.07829*, 2018.
- Wang, Y., Yi, K., Liu, X., Wang, Y. G., and Jin, S. Acmp: Allen-cahn message passing for graph neural networks with particle phase transition. *arXiv preprint arXiv:2206.05437*, 2022.
- Wu, Z., Pan, S., Chen, F., Long, G., Zhang, C., and Philip, S. Y. A comprehensive survey on graph neural networks. *IEEE Transactions on Neural Networks and Learning Systems*, 2020.
- Xu, K., Hu, W., Leskovec, J., and Jegelka, S. How powerful are graph neural networks? In *International Conference on Learning Representations*, 2019. URL <https://openreview.net/forum?id=ryGs6iA5Km>.
- Zhao, K., Kang, Q., Song, Y., She, R., Wang, S., and Tay, W. P. Graph neural convection-diffusion with heterophily. In *Proc. International Joint Conference on Artificial Intelligence*, Macao, China, Aug 2023.
- Zhu, J., Yan, Y., Zhao, L., Heimann, M., Akoglu, L., and Koutra, D. Beyond homophily in graph neural networks: Current limitations and effective designs. *Advances in Neural Information Processing Systems*, 33:7793–7804, 2020.

A. BPGNN Architecture

We now provide details on the implementation of our BPGNN, which combines concepts of reaction-diffusion similar to (Wang et al., 2022; Choi et al., 2023) and our proposed QUBO aware node features.

Overall, our BPGNN is defined by the following ordinary differential equations (ODE) and initial conditions:

$$\dot{\mathbf{h}} = -\mathbf{L}(\mathbf{h} + \mathbf{r})\Sigma(t) + f(\mathbf{h}, t; \boldsymbol{\theta}(t)) \quad (24)$$

$$\mathbf{r}(\mathbf{h}, \mathbf{A}, \mathbf{b}; t) = q(\mathbf{h} \odot (\mathbf{A}\mathbf{h} + \mathbf{b}); t) \quad (25)$$

$$\mathbf{h}(t=0) = \mathbf{h}_0 = \text{enc}(\mathbf{b}) \quad (26)$$

Here, $\mathbf{h}(t) \in \mathbb{R}^{k \times d}$ is a hidden feature matrix with d features that depends on the initial state \mathbf{h}_0 , and the input node features $\mathbf{b} \in \mathbb{R}^{k \times 1}$. $\dot{\mathbf{h}} = \frac{d\mathbf{h}(t)}{dt}$ denotes the first-order derivative with respect to time. \mathbf{L} is the graph Laplacian as in (Eliasof et al., 2021). \mathbf{r} is a continuous version of the QUBO objective aware features as shown in Equation (14), and q is an MLP. The initial state is obtained by embedding the input node features using a single layer MLP; $\mathbf{h}_0 = \text{enc}(\mathbf{b})$. Also, $\Sigma(t) \geq 0$ is a diagonal matrix with non-negative learnable diffusion coefficients on its diagonal. The reaction term f from Equation (24) is a learnable point-wise non-linear function that depends on the current hidden state $\mathbf{h}(t)$.

In order to obtain a graph neural layer from Equation (24)-(26), we use the forward Euler discretization method, as is common in GNNs (Eliasof et al., 2021; Chamberlain et al., 2021; Gravina et al., 2022). Therefore, a BPGNN layer is defined by the following update rules shown in Algorithm 2.

Algorithm 2 BPGNN Layer

Input: Node features $\mathbf{h}^{(\ell)} \in \mathbb{R}^{k \times d}$

Output: Updated node features $\mathbf{h}^{(l+1)} \in \mathbb{R}^{k \times d}$

- 1: Compute QUBO Aware node features:
 $\mathbf{r}^{(\ell)} = \mathbf{h}^{(\ell)} \odot (\mathbf{A}\mathbf{h}^{(\ell)} + \mathbf{b})$
 - 2: Diffusion:
 $\mathbf{h}^{(l+1/2)} = \mathbf{h}^{(\ell)} - \epsilon\mathbf{L}(\mathbf{h}^{(\ell)} + g^{(\ell)}(\mathbf{r}^{(\ell)}))$.
 - 3: Reaction:
 $\mathbf{h}^{(l+1)} = \mathbf{h}^{(l+1/2)} + \epsilon f(\mathbf{h}^{(l+1/2)}; \boldsymbol{\theta}_r^{(\ell)})$.
 - 4: Return $\mathbf{h}^{(l+1)}$.
-

B. Metrics

We now discuss the three metrics reported in our experiments, in Section 7.

Solution Accuracy (%). The solution accuracy measured the number of correctly labeled nodes in each example. Mathematically, given a graph $G = (V, E)$, with n nodes, predicted solution \mathbf{x}_p and ground-truth solution \mathbf{x}_o , the ac-

curacy is defined as follows:

$$\text{Accuracy} = \frac{\sum_{i=0}^{n-1} \mathbb{1}_{\mathbf{x}_{o_i} = \mathbf{x}_{p_i}}}{n}, \quad (27)$$

where \mathbf{x}_{o_i} denotes the i -th entry of \mathbf{x}_o , and similarly for \mathbf{x}_{p_i} . $\mathbb{1}_{\mathbf{x}_{o_i} = \mathbf{x}_{p_i}}$ is an indicator function that reads 1 if the equality between the entries holds, and 0 otherwise.

Relative QUBO Objective. Recall the QUBO objective from Equation (1). At the optimal solution \mathbf{x}_o , its value reads:

$$f_0 = f(\mathbf{x}_o; \mathbf{b}, \mathbf{A}) = \mathbf{x}_o^\top \mathbf{A}\mathbf{x}_o + \mathbf{x}_o^\top \mathbf{b}. \quad (28)$$

Similarly, we measure the QUBO objective at the predicted solution \mathbf{x}_p :

$$f_p = f(\mathbf{x}_p; \mathbf{b}, \mathbf{A}) = \mathbf{x}_p^\top \mathbf{A}\mathbf{x}_p + \mathbf{x}_p^\top \mathbf{b}. \quad (29)$$

We then define the *relative* QUBO objective as follows:

$$\text{RelQUBO} = \frac{f_p - f_o}{|f_o|} \quad (30)$$

Note that since f_o is the optimal value in this minimization problem, it is always true that $f_p \geq f_o$, and therefore the lowest and best value of this metric is 0.

Inference time. We measure the time it takes for each approach (exhaustive search, classical solvers, other GNNs, and ours) to solve a QUBO problem. The time is measured in milliseconds and averaged over the solution of 100 problems with the same size per dataset. The measurements were conducted using an Nvidia RTX-4090 GPU.

C. Datasets

We create 3 datasets: small ($k = 10$), medium ($k = 256$), and large ($k = 1024$). For the small dataset, we generate exact solutions using an exhaustive search, with 1 million examples. For the small and medium examples, we generate 1000 examples using the procedure described in Algorithm 1. Since we consider problems where \mathbf{A} is fixed but the observed-vector \mathbf{b} is variable, we repeat the process of generating datasets 10 times, so that we have examples on several randomly generated matrices \mathbf{A} . The results in Section 7 are averaged across the 10 datasets, following the common experimental settings in Xu et al. (2019). In all cases, we employ a random training/validation split of 80%/20%, respectively.

For the medium and large datasets, we chose \mathbf{A} to be the matrix that discretizes the 2D Laplacian on a lattice. Such matrices often appear in thermodynamics calculations (Evans, 1998). The data is generated using algorithm 1. In order to make the problem non-trivial, we choose $\sigma = 4$ which makes roughly 5% of the entries in \mathbf{x}_o change. We have used 1000 Tabu search steps in step (4) of the algorithm to approximate \mathbf{x} .

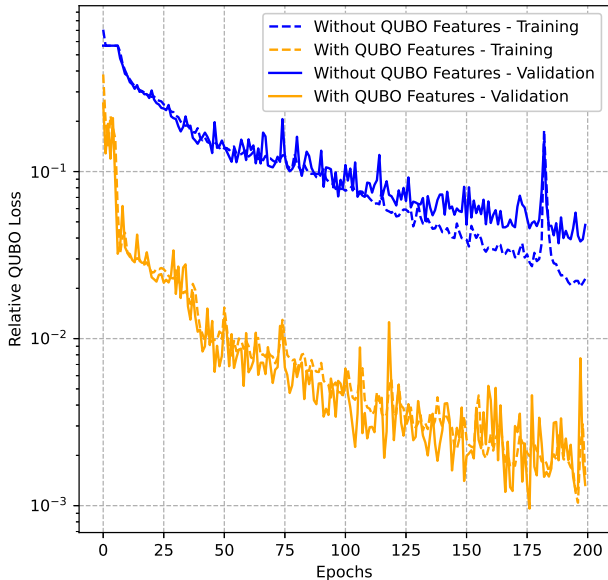


Figure 3. The *relative QUBO loss* convergence in training and validation of BPGNN on the small problem ($k = 10$), with and without the QUBO-aware node features from Equation (14).

D. Hyperparameters

In our experiments we consider the following hyperparameters for all GNN methods, including ours: $\text{learning_rate} \in \{1e-5, 1e-4, 1e-3\}$, $\text{weight_decay} \in \{1e-5, 1e-4, 0\}$, $\text{dropout} \in \{0, 0.1, 0.5\}$. We train each network for up to 200 epochs. Dropout layers, if used, are applied after each hidden layer. We used the Adam (Kingma & Ba, 2014) optimizer in all experiments.

For the classical solvers, we used up to 1000 iterations, with early stopping if the objective function does not improve after 50 iterations, with both TS and SAB methods. We start the algorithms from an initial guess of zeros, as is standard.

E. Additional Results

E.1. Standard Deviation of the Relative QUBO Loss

Due to space constraints, we provide the obtained relative QUBO loss standard deviations of the various methods in Table 3.

E.2. The Importance of QUBO-Aware Features

We now provide additional results on the importance of including the QUBO-aware features, on small and medium-sized problems, in Tables 4 and 5, respectively. As discussed in Section 7.2, the results indicate that including the QUBO-aware features improves accuracy and the relative QUBO

objective.

Furthermore, as we show in Figure 3, a beneficial property of the QUBO-aware features is their ability to accelerate the training convergence of the network.

Graph Neural Networks for Binary Programming

Method ↓ / Problem Size →	Small ($k = 10$)	Medium ($k = 256$)	Large ($k = 1024$)
CLASSICAL SOLVERS.			
TS	$5.90 \cdot 10^{-3} \pm 1.45 \cdot 10^{-6}$	$4.72 \cdot 10^{-3} \pm 5.38 \cdot 10^{-6}$	$4.58 \cdot 10^{-3} \pm 2.25 \cdot 10^{-5}$
SAB	0	$5.38 \cdot 10^{-2} \pm 3.91 \cdot 10^{-4}$	$7.96 \cdot 10^{-2} \pm 7.23 \cdot 10^{-4}$
GNN BASELINES.			
GCN	$7.12 \cdot 10^{-1} \pm 1.29 \cdot 10^{-2}$	$5.03 \cdot 10^{-1} \pm 3.60 \cdot 10^{-2}$	$8.76 \cdot 10^{-1} \pm 7.21 \cdot 10^{-2}$
GAT	$6.98 \cdot 10^{-1} \pm 3.96 \cdot 10^{-2}$	$4.38 \cdot 10^{-1} \pm 5.78 \cdot 10^{-2}$	$7.23 \cdot 10^{-1} \pm 8.35 \cdot 10^{-2}$
GCNII	$5.67 \cdot 10^{-1} \pm 1.10 \cdot 10^{-2}$	$4.13 \cdot 10^{-1} \pm 2.17 \cdot 10^{-2}$	$5.08 \cdot 10^{-1} \pm 4.93 \cdot 10^{-2}$
Dir-GNN	$3.74 \cdot 10^{-2} \pm 5.85 \cdot 10^{-3}$	$1.07 \cdot 10^{-1} \pm 9.91 \cdot 10^{-3}$	$9.62 \cdot 10^{-2} \pm 9.97 \cdot 10^{-3}$
OURS.			
BPGNN	$2.83 \cdot 10^{-3} \pm 4.48 \cdot 10^{-4}$	$5.31 \cdot 10^{-3} \pm 5.92 \cdot 10^{-4}$	$1.26 \cdot 10^{-2} \pm 5.47 \cdot 10^{-3}$
BPGNN + TS	$1.37 \cdot 10^{-5} \pm 2.77 \cdot 10^{-6}$	$1.21 \cdot 10^{-5} \pm 3.81 \cdot 10^{-6}$	$1.10 \cdot 10^{-4} \pm 7.09 \cdot 10^{-6}$

Table 3. The Relative QUBO loss (lower is better) average and standard deviations over 10 experiments, using various naive exhaustive search methods, classical methods, GNNs, and our BPGNN.

QUBO Features	Small ($k = 10$)		
	Acc(%)	Rel QUBO Objective	Inference Time (ms)
✗	$97.0_{\pm 0.6}$	$2.18 \cdot 10^{-2}$	2.7
✓	$98.2_{\pm 0.5}$	$2.83 \cdot 10^{-3}$	2.8

Table 4. The impact of adding the QUBO aware features from Equation (14) to the node features on small sized problems ($k = 10$).

QUBO Features	Medium ($k = 256$)		
	Acc(%)	Rel QUBO Objective	Inference Time (ms)
✗	$95.9_{\pm 0.4}$	$6.14 \cdot 10^{-2}$	2.9
✓	$97.2_{\pm 0.5}$	$5.31 \cdot 10^{-3}$	3.0

Table 5. The impact of adding the QUBO aware features from Equation (14) to the node features on medium sized problems ($k = 256$).